https://doi.org/10.37434/tpwj2021.04.06

# METHOD OF ACOUSTIC EMISSION AT EVALUATION OF THE STATE OF WELDS AND THEIR SERVICE PROPERTIES. Part 2. PRACTICAL APPLICATION

**S.A. Nedosieka, A.Ya. Nedosieka, M.A. Yaremenko, O.I. Boichuk** and **M.A. Ovsienko**
E.O. Paton Electric Welding Institute of the NAS of Ukraine
11 Kazymyr Malevych Str., 03150, Kyiv, Ukraine. E-mail: inpat59@paton.kiev.ua

The majority of existing structures contain welded joints. Questions of monitoring service characteristics of welded joints, using acoustic emission method, are considered. Attention is given to a change in material properties of operating structures with welded elements after long-term service, taking into account the time and probable violation of service conditions. Examples of evaluation of the change in properties of welded structure materials by the data of acoustic emission, determination of their damage and residual service life, are given. 17 Ref., 5 Tables, 24 Figures.

*Keywords: welds, service properties, acoustic emission (AE), AE activity, AE scanning, damage, destruction*

Influence of the type of welded joint on acoustic emission (AE) and possibility of quantitative evaluation of such an influence by AE method was considered in part 1 of this paper [1].

High sensitivity of AE method to defect initiation and propagation in materials at very early stages of destruction allows controlling the service properties of welded joints both directly during welding, and at any stages of welded structure operation [2].

Part 2 deals with the questions of practical application of AE method for welding process control and evaluation of service properties of different types of welded joints in the case of some structures with prolonged operating period. Note that the load-carrying ability of the structure and its service life are largely formed at the fabrication stage. Correction of the above factors occurs during routine or unscheduled repairs. As the majority of metal structures are welded, their quality essentially depends on the state of welds, in particular, those made during repair. Fracture in a gas pipe along the incomplete penetration line due to the arc shifting during welding, can be given as an example of poorly performed weld (Figure 1).

An important element, in terms of preventing the situations similar to those presented in Figure 1, is the possibility of controlling by AE method the weld quality directly during welding. Such experiments were conducted at PWI, and they showed that AE method allows rejecting the poor quality areas of welds on steel samples during welding.

In order to demonstrate the applicability of AE method to control defect initiation during welding of aluminium alloys we will perform studies of AMg5V alloy. A plate of 10 mm thickness was welded, weld dimensions were 600×12 mm. ADSV-2 unit was used for welding. Welding was performed by tungsten electrode with 2 mm filler wire from AMg6 alloy. Welding parameters were as follows: voltage $U$ = 16 V, cur-

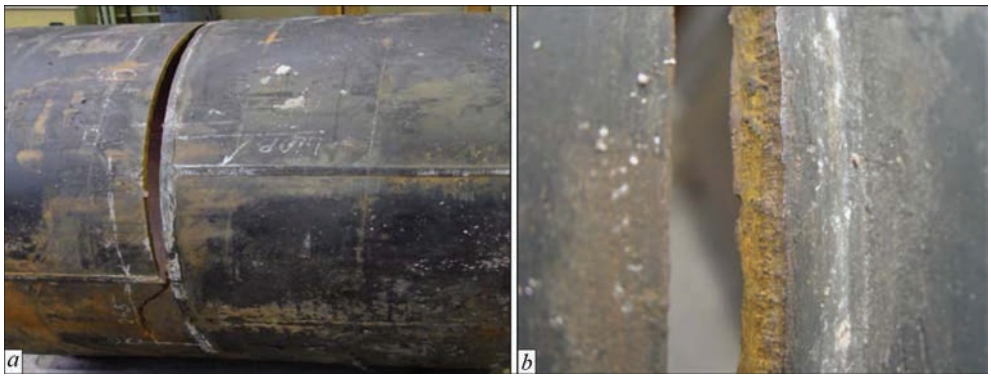

**Figure 1.** Gas pipe after destruction (*a*) and enlarged image of an area, which shows the result of incomplete penetration of metal (*c*)

S.A. Nedosieka — https://orcid.org/0000-0002-3239-381X, A.Ya. Nedosieka — https://orcid.org/0000-0001-9036-1413,
M.A. Yaremenko — https://orcid.org/0000-0001-9973-4482, O.I. Boichuk — https://orcid.org/0000-0001-5800-1549,
M.A. Ovsienko — https://orcid.org/0000-0002-2202-827X

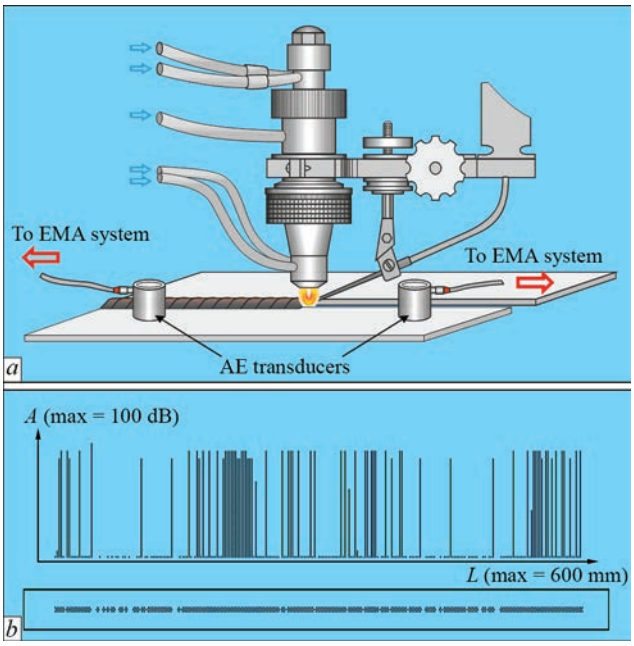


**Figure 2.** Investigation of AMg6 alloy: *a* — scheme of plate welding; *b* — histogram of amplitudes *A* of *AE* events along the weld, relative to coordinate *L* (top) and coordinate of these AE events (bottom)

rent $I$ = 350 A, arc movement speed 15 m/h. AE was recorded using EMA-1 system based «Defectophone» measuring device and two transducers of DAE-01 type, located at the ends of the welding zone, that allowed obtaining the coordinates and amplitudes of AE events arising during welding. The pattern of distribution of AE events and their amplitudes are given in Figure 2, *b*. By the data of investigations conducted after welding, weld quality was satisfactory, no defects inadmissible for service conditions were found. At the same time (Figure 2, *b*) a large number of AE events with high amplitudes were registered during testing. Accordingly, we can assume that AE system registered slight damage of the type of dislocation shifts, or similar ones. It means that coarser defects can also be registered, but filters have to be developed and applied for rejecting the obtained AE signals by certain criteria, extracting from them the events corresponding to the presence of really dangerous defects. It requires additional studies.

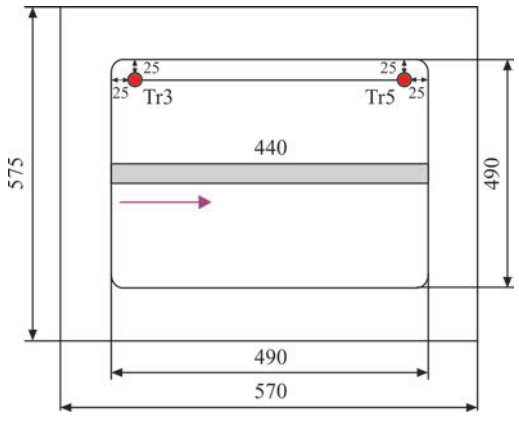


**Figure 3.** Typical scheme of steel plate welding testing

In order to solve the set tasks for steels, welding of three samples from 09G2S material and of two samples from 13KhGMRB (material prone to defect formation) was conducted. Sample thickness was 20 mm. Locations of mounting AE transducers were determined and prepared beforehand, and their protection during welding was provided. Control was performed using EMA-2 system, and data was processed with EMA-3.92 software (SW) [3]. Before conducting AE testing, preliminary test sounding was performed to determine the initial data, required for EMA-2 system operation: fixed threshold — 10 mV; floating threshold — 2σ; measurement dead time — 10 ms; high-frequency filter cutoff frequency — 100 kHz. AE testing was conducted both during welding in order to evaluate AE levels, taking into account the impact of technological obstacles, evaluation of the impact of multipass and poor welding on the general AE pattern, and during the weld cooling.

During performance of AE testing, the discrete and continuous AE is registered. Discrete AE characterizes crack propagation, transition of structural material into the ductile state, opening of oxide films, etc. The mechanism of discrete AE generation is initiation of damage in the material structure and its discrete development. Continuous AE characterizes fluid or gas flowing out through discontinuities in the material or intensive displacement of dislocation groups. The mechanisms of continuous AE generation are processes of continuous local rebuilding of the material structure at their deformation or seepage and flowing out of fluids and gases through discontinuities and cracks.

Two transducers (channels Nos 3, 5 for 09G2S steel and Nos 1, 2 — for 13KhGMRB) were used to determine the coordinates of AE sources. Cluster location was used. The size of the cluster for recording the zones of higher AE activity during welding was determined as 10 % of that of the array base, which was 100–420 mm. Clustering of the registered events from acute discontinuity, such as a crack, is continuous, while the plastic deformation regions associated, for instance, with corrosion damage, form an area of the source with a high degree of indeterminateness in size. In most cases the growing crack is regarded as the most hazardous defect. The sources which are considered as low-active or low-intensive ones usually do not require further assessment.

The overall testing scheme is given in Figure 3 (other schemes differ only by the plate width and distance between AE transducers).

Let us focus on the most revealing research results. The main and most basic result is that a clear

**Table 1.** Parameters of welding 09G2S steel plates

| Pass number | Welding parameters | | |
|---|---|---|---|
| | $I$, A | $U$, V | $V_w$, m/h |
| 1 | 220-230 | 36-37 | 16–17 |
| 2 | 250 | 35-36 | 20 |
| 3 | 250 | 35 | 20 |
| 4 | 250 | 35 | 16–17 |
| 5 | 250 | 35 | 19–20 |

AE pattern is obtained during welding, irrespective of the number of passes and weld quality, while the registered events follow the welding process. AE parameters and pattern during five pass welding (restrained butt joint) are given in Table 1 and Figure 4. Results of radiographic testing performed after weld cooling, show that welding quality was satisfactory (Figure 5).

Figure 4 presents the fragments of location screens of EMA-3 program, where the lower part shows the location scheme with transducer numbers, and given under it are the coordinates of registered AE events (vertical lines, the height of which corresponds to event amplitude of 0–500 mV). Above the location scheme the clusters based on AE events are shown by bars with flags (bar colour corresponds to a certain amplitude of AE events, the flag shows the number of AE events in the respective cluster). This description also applies to Figures 7, 21 and 23.

AE pattern during the first and fifths welding passes (Figure 4) differs only slightly both by the number of AE events, and by their location (the pattern was largely identical during the other three passes). The nature of location of the formed clusters is stochastic, in keeping with the stochastic nature of AE signal generation during welding, and as such they do not carry any essential information on welded joint quality. However, the standards of sound welding process can be in principle created on their base.

The next important result is the fact that as the sample cools after welding; the number of registered AE events gradually decreases and reaches zero mark even before the complete cooling of the weld. The time for disappearance of AE data after completion

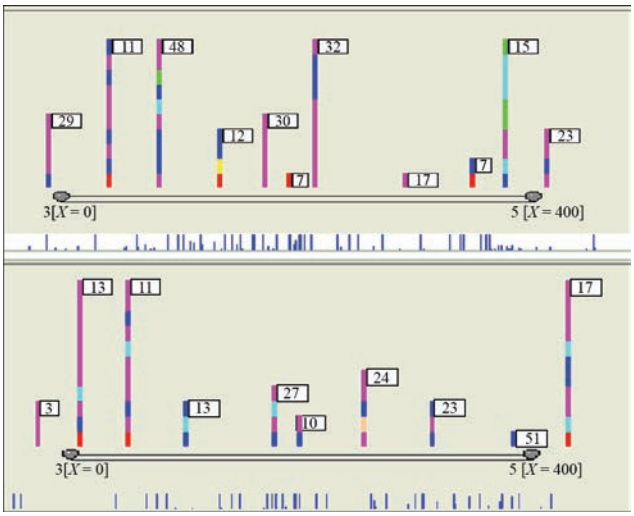


**Figure 4.** Photos of EMA system location screen. First (top) and last (below) stages of welding plates acc. to Table 1

of the welding process can be used as a criterion of its quality. For instance, in the above-described experiment where weld quality is rather high, a rapid reduction of the number of AE events was observed with cooling, and at lowering of weld temperature to 48 °C — their complete absence further on.

Behaviour of 13KhGMRB material can be characterized in a quite different way. During welding with ANP-2 electrode ($d$ = 4.0 mm) AE activity similar to that found in 09G2S steel was observed, but a crack approximately 100 mm long initiated in the material (Figure 6). This resulted in recording AE events in the crack vicinity on the second day after welding (Figure 7). Transducers 1 and 2 here were located close to the crack edges.

Despite the slight acoustic activity, its very presence after the complete cooling of the sample shows that the AE method is highly sensitive to defects, the development of which was not completely inhibited after completion of the welding process and subsequent complete cooling of the sample to room temperature.

Thus, one of the features of welded joint quality is AE absence after complete cooling of the weld, and the time for AE disappearance can serve as a quantitative characteristic of welding quality (material sound-

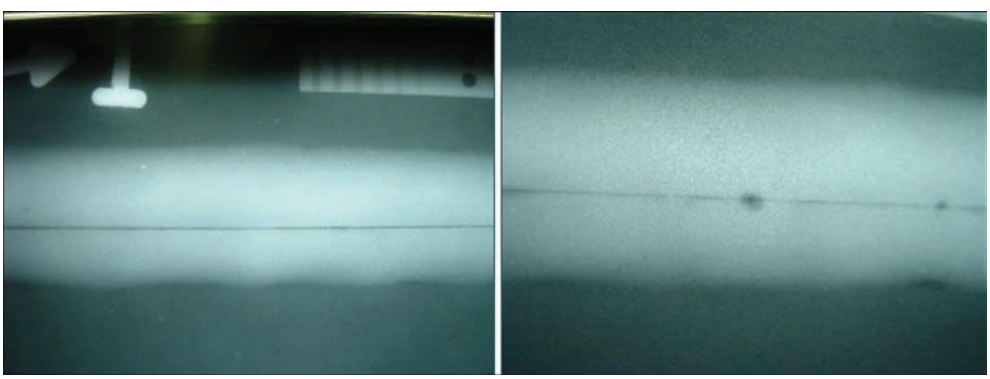

**Figure 5.** Radiography of individual weld areas after five welding passes

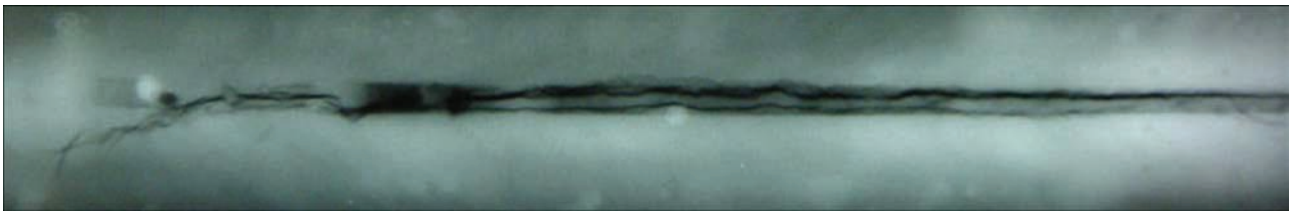

**Figure 6.** Radiography of a crack in as-welded 13KhGMRB material

ing can continue also after cooling, sounding time depends on the material).

As the scope of this series of experiments on AE testing of the welding process was quite limited, continuation of such studies should be recommended, as in case of obtaining results which could be used in production, it would allow a significant improvement of welded product control directly during its manufacture. Note also that such research has been more actively pursued abroad lately [4–6, 12–13].

Let us consider the possibility of AE testing of large-sized structures by a small number of AE transducers. As a rule, such structures contain a large number of welds. A feature of local structures is the fact that many of them have exhausted their planned service life, but for economic reasons they cannot be replaced completely, or even partially. The only method to continue their safe operation is periodic inspection or continuous monitoring. Here, there is no other nondestructive method, besides AE, which would allow performing 100 % control of such structures with a small number of samples. At the same time, testing results obtained by AE method can be effectively verified by other methods due to the fact that AE application allows localizing the dangerous areas with rather high accuracy, and checking of the obtained data by other methods should be performed in them. This essentially accelerates the process of evaluation of the state of the structure being controlled, and, at the same time, allows verifying the reliability of AE testing results.

One of such demonstration trials was testing by AE method a coil of P-101 furnace of total length of about 1200 m that consists of four flows, which have the respective radiation and convection sections each. The coil is a pipe of 219 mm diameter and 10 mm thickness and is an increased danger facility, as the pipe wall temperature can be up to 523 °C, working pressure is 60 atm, and the working medium is explosive vacuum distillate. The total number of welds is close to 500. Note that complete control of the entire surface of the coil by other nondestructive testing methods would have required hundreds of times longer period and complex preparatory operations. Now in this case, in order to perform the testing, it was necessary to scrape and degrease four areas of 13 mm diameter to mount transducers on them (Figure 8) and fasten them by a special acoustically transparent couplant. Previous check showed a slight attenuation of AE signals in the material (12Kh18N10T steel); so that it was possible to conduct complete testing of the coil in just 2 stages of 600 m each. This is indicative of an essential advantage of the AE method in terms of time and effort consumption, compared to other nondestructive methods, as well as of the possibility in principle of performing 100 % testing of the object state with a small number of transducers without the need to move them to other locations during testing.

Loading was applied by a procedure standard for AE testing — pressure increase up to 20 atm with subsequent soaking for 10 min, then again pressure increase and soaking, repeating it several times up to maximum test pressure of 60 atm. Testing procedure here took about 100 min.

As the results of the conducted coil testing have already been published [7], let us focus on the derived conclusions. They are important, as after AE testing the critical locations indicated by AE method, were checked by independent experts, using two nondestructive methods — dye penetrant flaw detection and radiography, which can be efficiently used to check

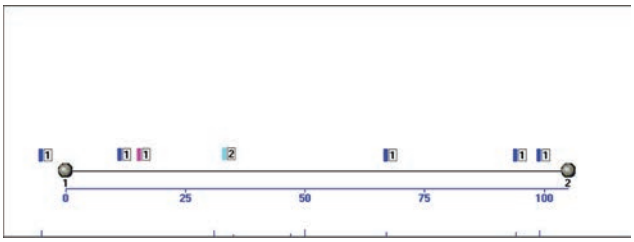


**Figure 7.** Photo of EMA system location screen (data on the next day after welding (13KhGMRB))

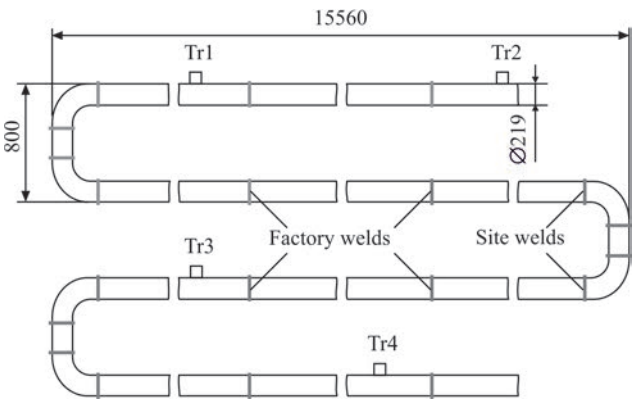


**Figure 8.** Scheme of location of welds and AE transducers (D1–D4) during coil testing

**Table 2.** Results of AE testing of the first flow confirmed by dye penetrant and radiographic flaw detection

| Area | Crack | | Pore | | Undercut | |
|---|---|---|---|---|---|---|
| | Quantity | Max. length/depth, mm | Quantity | Max. dia, mm | Quantity | Max. length, mm |
| Radiation | 2 | 4/2 | 2 | 2 | 1 | 300 |
| | 1 | 60/3 | 2 | 2 | 3 | 200 |
| | 3 | 8/3 | 3 | 3 | 2 | 200 |
| | 2 | 5/2 | – | – | 1 | 100 |
| | 2 | 6/3 | – | – | – | – |
| | 2 | 8/3 | – | – | – | – |
| Convection | 2 | 6/2 | 3 | 2 | – | – |
| | 4 | 8/2 | – | – | – | – |
| Transition | – | – | 2 | 3 | 1 | 60 |

the AE data [8]. It allowed confirming the high reliability of AE data, as well as determining the defects which were exactly the cause for AE event generation. For greater clarity, let us give in Table 2 just the data obtained for the first flow.

As we can see most of the defects found in welds are cracks, followed by pores, and the number of found undercuts is the smallest. This statistics typical for all the four flows, suggests that the AE method can be used with success to control the service properties of large-sized welded structures, which are also potentially dangerous for the environment. This is the most important conclusion, but the derived data further allow assessing how useful could be the continuous AE monitoring of this facility. Table 2 shows that the pipe continued to operate with a crack in the weld, which was 60 mm long and 3 mm deep, i.e. almost one third of the pipe thickness. A probable cause for the pipe not breaking can be the static indeterminateness in the location close to this weld. Structures with such a feature can go on operating for years in the presence of rather large cracks (for instance, bridge, truss and crane structures). Results of metallographic examination of typical weld defects are given in Figure 9.

Then the following question arises: how can we determine that the crack poses a threat for the structure at this stage of operation? There are a large number of calculation methods, including those based on fracture mechanics. In the case of correct definition of the problem and its solution by a competent specialist rather reliable result can be obtained. However, calculations take time, which may be lacking during the real operation of the structure, as destruction may take place earlier. An alternative to calculations is continuous AE monitoring, using standardized and certified methods of danger assessment and prediction of breaking load. At continuous monitoring, any development of a defect dangerous for the structure, will be recorded in advance, which will be followed by the system giving a colour and sound hazard signal about in real time, and the screen will display the quantitative indices of breaking load prediction (Figure 14 [1]). This is a fast and safe method of accident prevention.

In this case the respective dangerous crack was detected by AE method as a propagating defect. The rapidity of crack development showed the need for repair of this dangerous section. Here, the overall dimensions of the dangerous defect and its location are not important for AE method. Only its acoustic activity matters. Now, application of additional control methods showed that the defect is indeed present, and allowed establishing its dimensions.

Repair of a certain number of welds was recommended, proceeding from the results of AE testing of P-101 furnace coil (Table 3).

The total number of rejected welds was 102. Considering that the total number of welds is equal to close to 500, let us approximately assess the integral

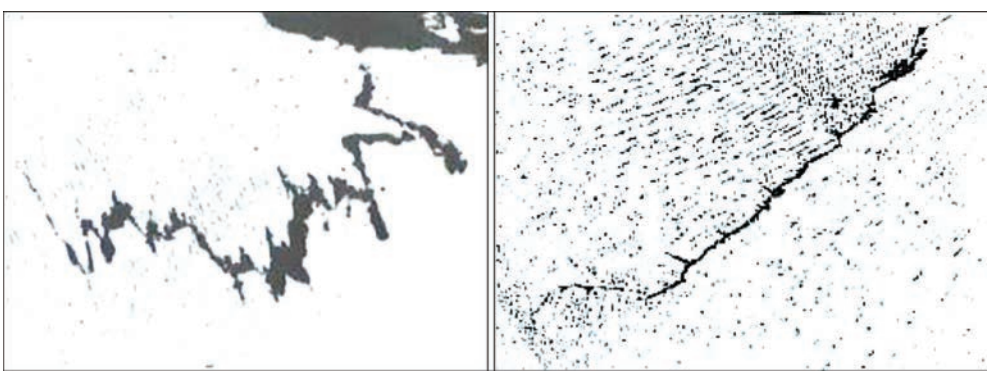

**Figure 9.** Typical cracks in P-101 furnace coil, ×120

**Table 3.** Recommended number of repaired areas of P-101 furnace coil by the results of AE testing

| Area | 1st flow | 2nd flow | 3rd flow | 4th flow |
|---|---|---|---|---|
| Radiation | 12 | 19 | 8 | 12 |
| Convection | 9 | - | - | 9 |
| Transition | 5 | 13 | 15 | - |
| Total | 26 | 32 | 23 | 21 |

damage of the object of control as a whole, using the ratio of the number of defective welds to their total number as the damage parameter [9, 10], in keeping with the following formula:

$$\Delta W_{av} = (1 - N_{dam}/N_{tot})\cdot 100\ \%, \quad (1)$$

where $\Delta W_{av}$ is the integral damage of the object of control; $N_{tot}$ is the total number of welds; $N_{dam}$ is the number of damaged welds, and we will obtain $\Delta W_{av} \approx 20$ %.

It is interesting to check the dependence of damage on operating life, considering that at the moment of testing the coil has operated for 15 years. The authors have obtained a generalized formula for arithmetic mean value of damage $\Delta W_{av}$ on a large number of pipes of the main gas pipelines, using five independent methods. It can be described [9] as:

$$\Delta W_{av} = ae^{bt}\cdot 100\ \%, \quad (2)$$

where $t$ is the operating life; $a = 0.1352$; $b = 0.0333$ [9].

Thus, for this object of control $\Delta W_{av}$ = 01352 exp(0.0333·15)·100 % ≈ 22 %. As we can see, the error at comparison of 20 % damage data calculated by testing results and their verification by formula (2) is negligible. The formula is used only for materials, which have been in service. It means that the generalized damage formula (1) is valid not only for pipes of the main pipelines, which operate under quite different loading and environmental conditions, but also for the tested furnace coil. Calculation of the residual life of the object at the moment of testing based on formula (2) will also be valid. This can be done using a nomogram (Figure 10), which correlates the residual life with damage [9–11]. The difference consists in that in the diagram the damage is expressed not in

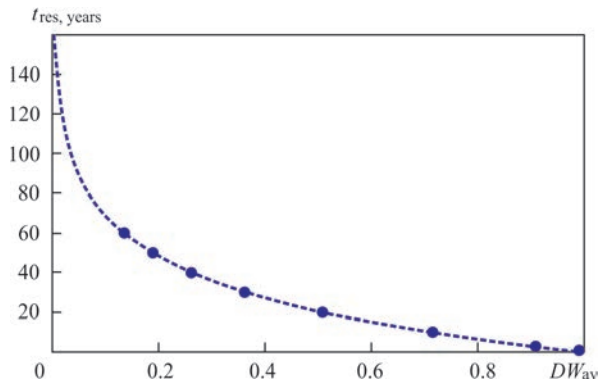


**Figure 10.** Nomogram for determination of residual life by known damage level

percent, but in fractions of a unity, and $\Delta W_{av} = 1$ corresponds to maximum damage.

It can be determined that at 20 % damage (or 0.2 in the nomogram) the integral residual life of the coil was ≈ 47 years at the moment of testing.

Thus, the results of AE testing of such facilities allow determination of dangerous sections, requiring repair, which include cracks, pores and undercuts of different dimensions and in different locations. Assessment of the obtained data allows evaluation of the integral damage of the objects of control and their residual life.

Note that despite the intensification of such research abroad [4–6, 12–16], their main disadvantage is absence of clearly normalized quantitative assessment of damage, prediction of destruction and probability. Here, it is dangerous to proceed from table data at evaluation of the state of both the base material and welded joint material, as even the adjacent sections of one and the same structure can have different physico-mechanical characteristics, different damage and different danger level, respectively. A rather promising local approach, which is also based on AE testing data, should be noted [17].

Large-scale testing of samples of pipeline materials from different regions of Ukraine with different operating time, conducted by PWI Department of Technical Diagnostics of Welded Structures, demonstrated an essential AE diversity, including differences in AE parameters:

- time of emergence of the first AE event (from 1 s to 2 min since the moment of testing start);
- loading, at which discrete AE appears (2–55 % relative to breaking load);
- level of continuous discrete AE (10–500 mV);
- oscillation of the level of continuous AE (2–1000 %);
- total number of AE events (7–12000);
- AE amplitude at the same deformation stages (1–500 mV);
- AE activity at the same deformation stages (1–100 $s^{-1}$);
- change of the number of AE events in materials with accumulated damage (from 2–10 times reduction to similar increase).

The above allows stating that no common AE pattern is found for the studied materials. However, the results of the conducted testing can be conditionally divided into 2 main groups [9]. The first group, which occurs more seldom, is characterized by reduction of the number of AE events in the material after many years of operation. The second, most characteristic group, differs by a significant increase of the number of events. Materials of the second group are characterized by a lower total level of AE amplitudes. Additional metallographic studies confirmed the assump-

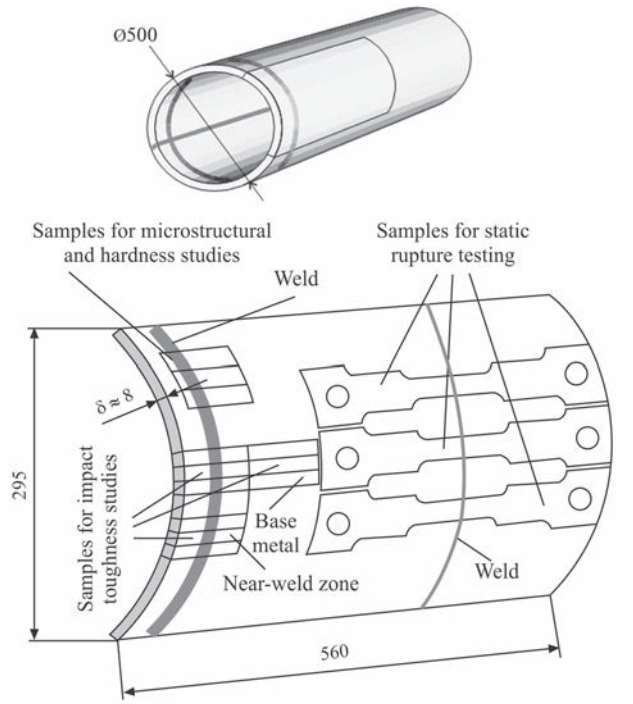


**Figure 11.** Scheme of cutting out samples from a test pipe fragment

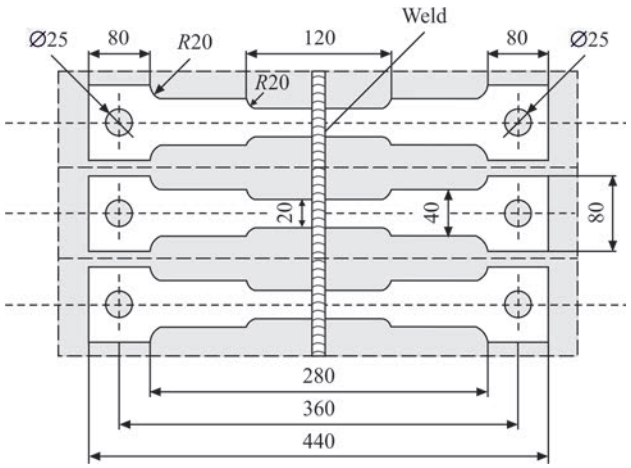


**Figure 12.** Scheme of cutting out AE-01R samples for AE studies at static tension

tion that for the first group the main change, associated with the operating time, is embrittlement, which leads to lowering of the number of AE events. For the second group, contrarily, increase in the number of AE events is indicative of accumulation of a large amount of scattered damage, that is confirmed by additional experiments conducted by four different methods and is the base at construction of AE model in ductile materials, where destruction develops by the mechanism of initiation, propagation and coalescence of a large number of pores. Such diversity leads to incorporating different parameters into the criterion (1), depending on the obtained AE data, in order to calculate the damage and residual life. Now, if the number of AE events almost does not change after a long operating period, it can be assumed that a mixed mode of damage accumulation is realized, namely embrittlement with simultaneous development of pores. At the same time, it should be noted that the algorithms of breaking load prediction, incorporated in SW of EMA type systems, perform with the same reliability, irrespective of the above-mentioned diversity of fracture modes.

We will demonstrate the effectiveness of evaluation of the state of material using the destruction prediction in the case of a pipe from the main pipeline, where an accident occurred earlier, and will compare the results with the data obtained by other methods. The material for investigations was taken from an area near the destruction location (pipe fragment with the weld closest to the destruction area). In keeping with the certificate, the pipe is made from steel 20 with 500 mm diameter and 8 mm wall thickness. Figures 11–13 show the schemes of manufacturing samples of different type for an integrated study of the properties of the obtained pipe fragment. Note that in Figure 11 the weld and samples in the right-hand part are shown conditionally for greater clarity. In reality, samples of AE-01R type were cut out of the same part of the pipe, as the others, from an area located to the left, so that the weld was in the middle of the sample (Figure 12). Samples of MI-50 type were used for determination of impact toughness of the material. Samples in the form of a rectangular parallelepiped were also prepared, which were used to study the material microhardness and to conduct AE scanning by

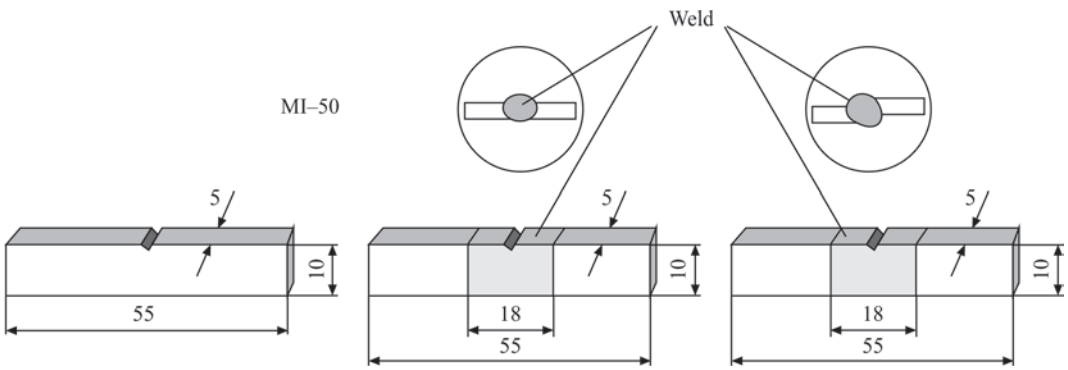


**Figure 13.** Scheme of preparation of MI-50 samples for impact toughness testing

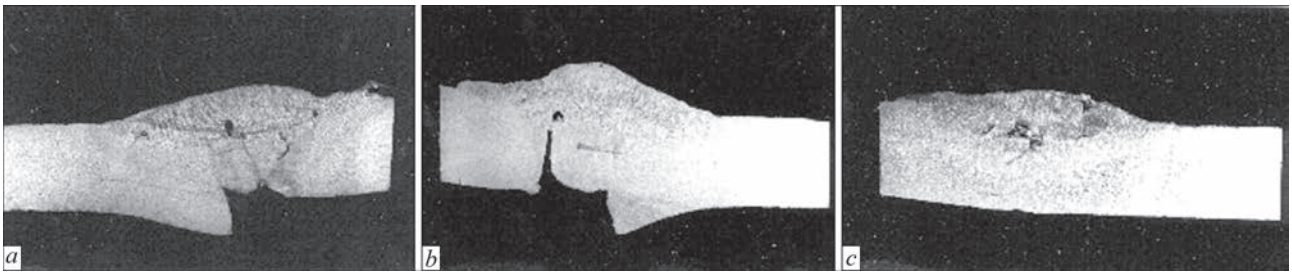

**Figure 14.** Weld macrostructure (×2.5). Samples I (*a*), II (*b*), III (*c*)

**Table 4.** Chemical composition of base metal and weld metal of the studied samples, wt.%

| Analyzed object | C | Si | Mn | Cr | Ni | Mo | V | S | P | [O] | [N] |
|---|---|---|---|---|---|---|---|---|---|---|---|
| Base metal | 00.137 | 00.138 | 00.40 | 00.05 | <0.05 | <0.03 | <0.02 | 00.013 | 00.009 | 00.02 | 00.073 |
| Weld | 0.129 | 0.430 | 0.90 | 0.06 | 0.05 | <0.03 | 0.03 | 0.020 | 0.017 | 0.043 | 0.011 |

one AE transducer emitting an acoustic signal from one end face of the parallelepiped and subsequent receiving of the modified signal by another transducer at the other end face [2, 9–11].

Macrostructural analysis was conducted after etching the samples in 20 % aqueous solution of ammonium sulphate. The microstructure was examined after etching in nital (4 % solution of nitric acid in ethyl alcohol). Investigations and filming of the microstructure were conducted in Polivar-met microscope. Hardness was measured by M-400 hardness meter of KOMPAS Company with the load of 25 gf (microhardness) and 1 kgf (integral hardness).

Chemical composition of base metal and weld metal is given in Table 4.

Chemical composition studies showed that the pipe material does not correspond to the specification and it is not steel 20. Proceeding from the results of chemical analysis of the studied samples and norms of chemical composition of steels, specified by GOST 1050-88, we can come to the conclusion that the pipe is made from steel 15 ps (semi-killed). Manufacturing pipes from such steels is allowed only under the condition that the gas pressure in them will not exceed 4 at. Visual examination of the welded template submitted for investigations, showed that the weld surface structure is coarse-layered with traces of repair welds over the entire weld length. Dents from the root side, lacks-of-penetration, and individual metal leakage are found in the weld root part practically along its entire length. Welds are porous, with individual slag inclusions and slag interlayers between the welds (Figure 14, *a*). The depth of the root lacks-of-penetration in individual cases reaches 50–60 % of thickness of the metal being welded (Figure 14, *b, c*). Welding was conducted with great edge misalignment (Figure 14, *c*) and a gap between them. Overlaps are present on the surface of the product being welded.

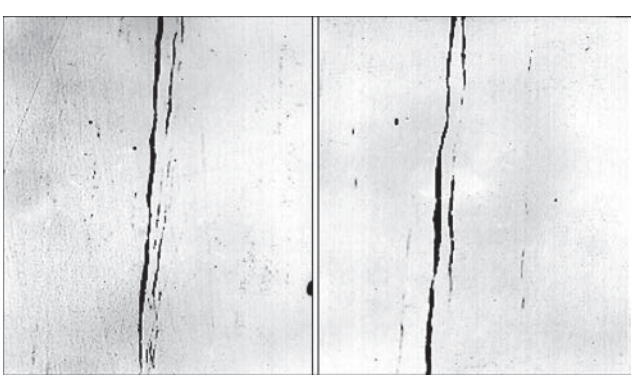

**Figure 15.** Nonmetallic inclusions in base metal (ductile silicates)

Contamination by nonmetallic inclusions was controlled in keeping with GOST 1778–70. Quantitative microscope of Omnimet model was used for their determination. It is found that the base metal is contaminated, mainly, by inclusions of the type of ductile silicates located mostly in the sample center (by the sheet thickness). Respective photos are given in Figure 15. The level of contamination by the above inclusions corresponds to 4.5 points to GOST 1778–70 (Sh1 method, SP scale). Calculation of the contamination showed that in the most contaminated locations the ductile silicate content was equal to 2.366 vol.%. Other inclusions (sulphides, oxysulphides) are contained in the base metal in very small amounts (less than point 1 to GOST 1778–70).

Oxides of globular-shaped inclusions of the size from several micrometers to submicrons were detected in weld metal (Figure 16). Quantitative analysis showed that the content of nonmetallic inclusions in the upper beads of samples I, II and III is equal to 0.156, 0.122 and 0.105 vol.%, respectively.

Defects and microstructure of various areas of the welded joint were studied in detail on microsections. Analysis showed that the base metal microstructure is the same on all the three samples. It consists of ferrite and pearlite with striation, corresponding to point 2 (GOST 5640–68) and ferrite grain size corresponding

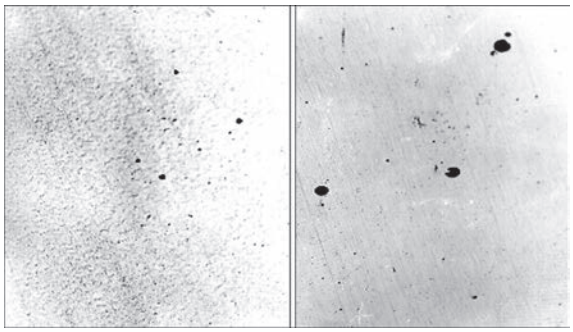

**Figure 16.** Nonmetallic inclusions (oxides) in weld metal

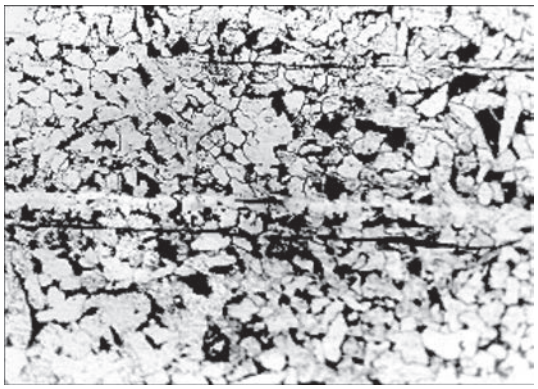

**Figure 17.** Base metal microstructure (×400)

to No.8 (GOST 5639–82). Figure 17 shows the photographs of base metal microstructure.

A characteristic feature of base metal structure is presence of a white band of heterogeneity in the sample center (in the direction of sheet thickness). It is known that segregation bands of this type are often saturated by carbon in quantities sufficient for martensite precipitation.

In the studied steel, however, the mentioned band consists of ferrite. This is confirmed, in particular, by measurements of microhardness, which, similar to respective microhardness of ferrite grains, is equal to Vickers *HV*–1180–1300 MPa. Integral hardness of base metal is here equal to *HV*–1450–1500 MPa. In sample 1 defects were studied at magnification greater than at macroexamination. Discontinuities were detected which can be characterized as pores (Figure 18). The microstructure of upper weld is a mixture of polygonal ferrite, pearlite and lamellar ferrite with disordered second phase (Figure 19, *a*). *HV* microhardness of these components is equal to 1100–1300, 2200 and 1700–1800 MPa, respectively. Integral hardness of the upper weld is equal to 1500–1600 MPa. At ×40 magnification a slag-filled root channel, macropores and micropores are visible (Figure 18).

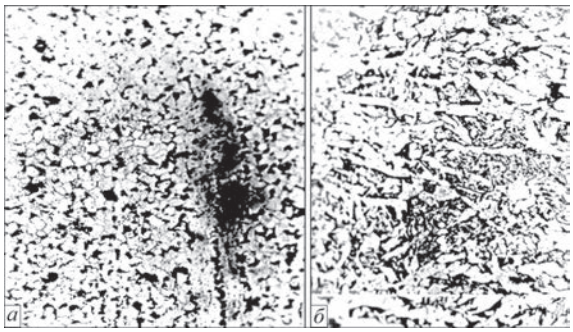


**Figure 19.** Microstructure (×400) of upper weld (*a*) and fusion zone of base metal with another weld (*b*)

The microstructure of the lower weld, subjected to heating at superposition of the upper weld, consists of mixed ferrite and pearlite (Figure 19, *b*). The same photo shows the zone of fusion with the base metal. One can clearly see that ductile silicates in the fusion zone have changed under the impact of the weld pool heat. No grain growth was detected in the overheated zone.

Analysis of the microstructure of sample III also showed presence of multiple defects in the welded joint metal. So, lacks-of-penetration in the form of a comma are observed near the pores, as well as extended lacks-of-penetration located mainly between the beads. Figure 20 gives the photos of the metal of a sample with lacks-of-penetration which pose a serious danger for the operated pipeline, as they significantly lower the strength of welded joints in the pipes. The microstructure and hardness of various areas of the welded joint in this sample does not differ from the microstructure and hardness of the previous samples in the respective areas.

It should be noted that no increase of the grain size in the overheated zones was observed in the HAZ of all the studied samples. In other areas of the HAZ,

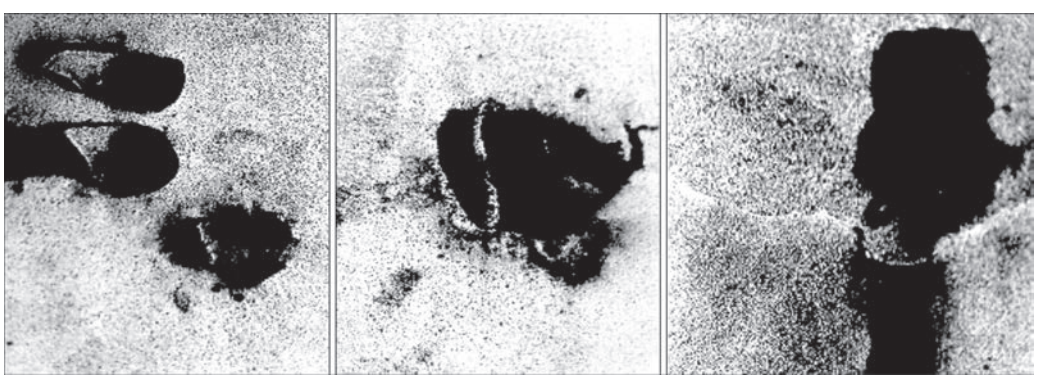

**Figure 18.** Pores in the weld of the sample (×40)

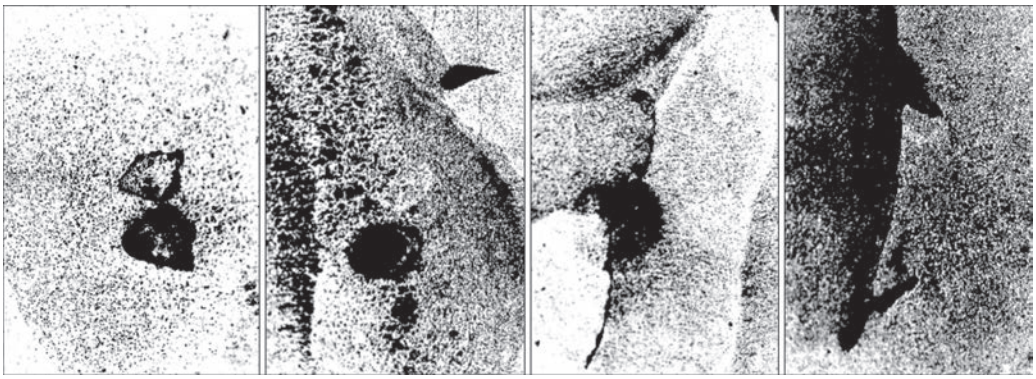

**Figure 20.** Defects in sample III (×40)

the metal structure consists of fine-grained ferrite and pearlite. Hardness of all the HAZ areas is not higher than 2000 MPa.

The general conclusion from chemical and metallographic analyses of the welds showed that multiple welding defects, as well as application of another steel grade instead of the design one led to destruction of the pipeline neighbouring section, but they could also cause destruction of the pipe fragment which was studied.

Material damage also demonstrates an essential lowering of impact toughness. For material in as-delivered condition it is equal to 218 J/cm$^2$. For MI-50 samples the data (Table 5) give a clear idea of both the state of the pipe base metal and of the welds.

As one can see, in the worst case the impact toughness decreased 2.5 times, while damage will be equal to 60 %, in keeping with formula (1).

AE scanning [2, 8–10] of three samples in the form of a parallelepiped showed that the maximum damage of the metal is observed in the direction normal to the pipe surface, and it is equal to 68 %. We will determine the strength of the material of the pipe, assuming that it is made from steel 20, to obtain the reference characteristics for comparison with the real material, from which the pipe is made. The initial parameters of the material are as follows: ultimate strength $\sigma_t$ = 440 MPa, yield limit $\sigma_y$ = 288 MPa, relative elongation $\psi$ = 28–34 %, reduction in area $\psi$ = 28–34 %, base metal impact toughness $[a_n]$ = 218 J/cm$^2$. Further on in the calculation we will denote the pipe wall thickness by value $\sigma$, regarding it as a thin shell ($r/\delta >> 10$).

**Table 5.** Impact toughness of pipe metal ($t_{test}$ = 20 °C)

| No | Pipe area | Impact toughness, J/cm$^2$ |
|---|---|---|
| 1 | Base metal | 187 |
| 2 | | 170 |
| 3 | | 165 |
| 4 | Weld | 155 |
| 5 | | 130 |
| 6 | | 88 |
| 7 | Weld with edge misalignment | 182 |
| 8 | | 155 |
| 9 | | 140 |

Pipe calculation can be performed, taking into account ratio $r/\delta$ = 41.34 >> 10 by the Laplace formula for a thin shell. According to the above formula, the stresses acting in the pipe, will be defined as $\sigma = pr/(2\delta_{ef})$, where $\sigma_{ef}$ is the real thickness of the shell wall. At selection of value $\sigma_{ef}$ it should be taken into account that only the thickness of lacks-of-penetration and other imperfections, changing the real wall thickness, should be subtracted from it, not forgetting also the fact that they are the stress raisers. The stress concentration factor $K$ for concentrators of such a shape is equal to 4.5.

Thus, with the specified pipe dimensions $\sigma$ = = 113.7 MPa, that is lower than $\sigma_y$ = 288 MPa. That is, when the material is in a nonembrittled state, the impact of stress concentration will lead to its redistribution in the raiser zone.

At material embrittlement, plastic deformations will be absent and $\sigma_{ef} = 113.7 \cdot 4.5 = 511.6$ MPa > $\sigma_t$. Thus, in the concentration zone the stresses will be higher than the ultimate strength and material destruction will take place. A recommended measure for preventing destruction is lowering the working pressure to 20–25 atm. As the material corresponds to steel 15 ps by its chemical composition and other characteristics, even lower performance is anticipated for it.

To complete analysis of service properties for this pipe, including the welds, we should analyze the results of AE studies of AE-01R sample for static tension. We will give typical screen images of EMA-3.92 program with the results of breaking load prediction and the respective graphs of testing samples from steel 20 first for material without any hours worked, taken from emergency stock (Figures 21–22), and then for the pipe material to be analyzed (Figures 23–24). All the elements of the location screen correspond to those described above for Figure 4 and in work [1]. Given above the location scheme are the results of breaking load prediction and their automatic conversion by EMA program to ultimate strength, according to the known


**Figure 21.** Screen of EMA-3.92 program after testing a typical sample of steel 20 from emergency stock


**Figure 23.** Screen of EMA-3.92 program after testing a typical sample of steel 20 with pipe damage

geometrical characteristics of the sample. In the graphs (Figures 22, 24) the bars show the amplitudes of discrete AE events (mV), loading *P* (kg) and total curve *N* of AE event accumulation, depending on testing time.

As we can see from Figure 21, the predicted ultimate strength fully corresponds to the specifications of steel 20. It should be also noted that the predicted breaking load, which in reality was equal to 9068 kg (Figure 22), corresponds to the requirements to its accuracy, according to the certificate for EMA type systems and falls within ± 15 %.

The graph (Figure 22) is characterized by the presence of a large number of events with maximum amplitudes. The curve of damage accumulation (total curve *N* of AE amplitudes) has a bend directed upwards, and it to a great extent follows the loading curve. As was reported in [1], this is an indication of absence of a welded joint in the sample.

For the tested sample from the damaged pipe, which, in addition had a weld, the predicted ultimate strength is significantly lower than the specifications of steel 20. It confirms, first, that another material was tested (as was already mentioned, this is steel 5ps), and secondly, that the material was damaged by the mechanism of pore initiation, development and coalescence with further cracking. Note that in this test also the predicted breaking load, which in reality was equal to 6576 kg (Figure 24), corresponds to the requirements to its accuracy and falls within the limits of ± 15 %.

Compared to the results of testing a sample from the emergency stock, the graph (Figure 24), is characterized by a small number of events, and they mostly have low amplitudes. The curve of damage accumulation (total curve *N* of AE amplitudes) has a bend, directed downwards, and does not follow the load curve that is indicative of the presence of a welded joint in the sample.

In keeping with formula (1) we will calculate the damage of a sample with the welded joint, compared to a reference sample from emergency stock. We will use the sum of events, *N*, as the damage parameter. After calculations, we will obtain the damage value of 73 %. The validity of such a damage level is indicated also by all the previous results, confirmed by metallurgical examinations.

As this damage value is the largest of those obtained for this pipe, we will use it for residual life assessment. In keeping with the nomogram (Figure 10), it is equal to ≈ 10 years for damage level of 0.73. Considering the large number of detected defects, the difference of the steel grade from the specification and probable destruction at overloading, it was recommended replacing the damaged pipe section with such values.

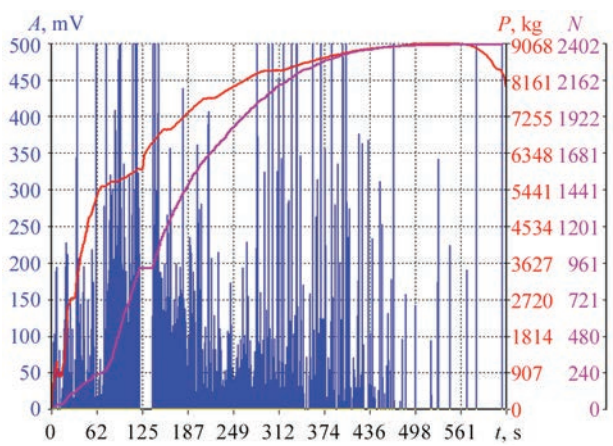


**Figure 22.** Graph of testing a typical sample of steel 20 from emergency stock

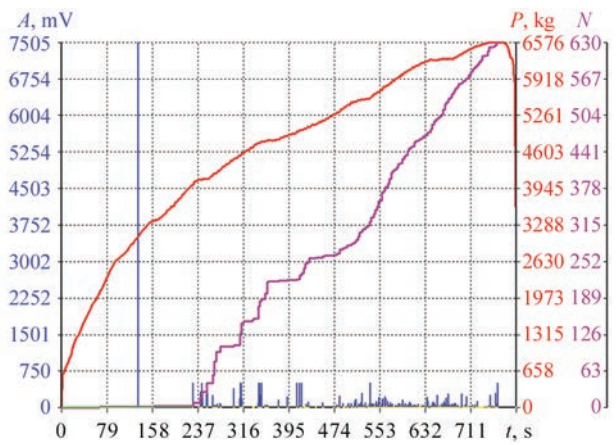


**Figure 24.** Graph of testing a welded sample from damaged pipe

Thus, integrated study of the material from an accident-prone pipe allows stating that AE method is sensitive to a change of service properties of welds, and at timely application it can help prevent emergency situations.

## Conclusions

1. The high sensitivity of AE method to initiation and propagation of defects of different types in welds, both during welding and during their further operation is demonstrated.

2. A characteristic, which could be used for quality control during welding, could be the time, during which acoustic activity disappears after welding is completed.

3. In the case of a coil of P-101 furnace it is shown that AE method is efficient during testing of large-sized potentially dangerous structures with a large number of welds. Here testing of large surfaces can be performed with a minimum number of transducers (four in this case). Additional testing methods are used to show exactly which defects are characteristic for different sections of the coil of P-101 furnace.

4. A method of integral assessment of damage of this type of facilities is proposed. Reverse check showed that the procedure of residual life calculation proposed by the authors is right for such facilities.

5. In the case of an emergency pipe section of the main gas pipeline, it is shown how an integrated assessment of damage level in base metal and welded joints can be performed with application of different methods. AE method was used to confirm the conclusion reached in Part 1 as to the possibility to determine the presence of a welded joint in the material by the angle of inclination of the total curve of AE events.

6. It is confirmed that breaking load prediction, performed by EMA type systems can be used for welded joints. It is shown that alongside the breaking load proper, its correct automatic conversion to ultimate strength is possible. Obtained results of conversion coincide with mechanical properties of the studied materials, determined by other methods.

7. Industrial application of AE technique is an efficient method to evaluate the service properties of welded joints that is highly important as they are one of the main causes for damage of structures in operation. Continuous AE monitoring provides the most reliable guarantee of prevention of emergency situations, as AE method immediately reacts to the smallest changes in the material state.


1. Nedoseka, S.A., Nedoseka, A.Ya., Yaremenko, M.A. et al. (2021) Acoustic emission method at evaluation of the state of welds and their service properties. Pt 1. Effect of welded joint type on acoustic emission. *The Paton Welding J.*, **2**, 46–52. https://doi.org/10.37434/as2021.02.09.
2. Nedoseka, A.Ya., Nedoseka, S.A. (2020) *Fundamentals of design and diagnostics of welded structures:* Manual. 5th Ed. Ed. by B.E. Paton. Kiev, Indprom [in Russian].
3. Nedoseka, A.Ya., Nedoseka, S.A., Yaremenko, M.A. et al. (2013) Software of AE diagnostic systems EMA-3.9. *Tekh. Diagnost. i Nerazrush. Kontrol*, **3**, 16–22 [in Russian].
4. Huang, W., Yang, S., Lin, D., Kovacevic, R. (2009) Real-time monitoring of the weld penetration state in laser welding of high-strength steels by airborne acoustic signal. ASME. Turbo expo: Power for land, sea, and air: cycle innovations; industrial and cogeneration; manufacturing materials and metallurgy. *Marine*, **4**, 799–805.
5. ASTM E749/E749M-17 (2017) *Standard practice for acoustic emission monitoring during continuous welding.* ASTM International, West Conshohocken.
6. Zhang, L., Basantes-Defaz, A.C., Ozevin, D. et al. (2019) Real- time monitoring of welding process using air-coupled ultrasonics and acoustic emission. *Int. J. Adv. Manuf. Technol.*, **101**, 1623–1634. https://doi.org/10.1007/s00170-018-3042-2.
7. Nedoseka, A.Ya., Nedoseka, S.A., Yaremenko, M.A. et al. (2003) About application of acoustic emission method for control of industrial structures. *Tekh. Diagnost. i Nerazrush. Kontrol*, **3**, 3–6 [in Russian].
8. Shcherbinsky, V.G., Feoktistov, V.A., Polevik, V.A. et al. (1987) *Methods of flaw detection of welded joints.* Moscow, Mashinostroenie [in Russian].
9. Nedoseka, S.A. (2010) *Diagnostics and prediction of service life of welded structures by acoustic emission method*: Syn. of Thesis for Dr. of Tech. Sci. Degree. Kyiv [in Ukrainian].
10. Nedoseka, S.A., Nedoseka, A.Ya., Boichuk, O.I. et al. (2020) Features of acoustic emission at evaluation of the state of materials. *Tekh. Diagnost. i Nerazrush. Kontrol*, **2**, 3–12 [in Ukrainian]. https://doi.org/10.37434/tdnk2020.02.01.
11. Nedoseka, S.A., Nedoseka, A.Ya. (2010) Integrated assessment of damage level and residual life of metals with certain operating life. *Ibid.*, **1**, 9–16 [in Russian].
12. Karlov, S.A., Sulzhenko, V.A., Yakovlev, A.V. (2019) Acoustic emission control of weld quality in marine engineering: *Transact. of Krylov State scientific center.* Special Issue [in Russian].
13. Ivanov, A.B., Ievlev, V.A., Neustupov, A.S. et al. (2019) Implementation of a new method for quality control of field welded joints of pipelines: *Transact. of Krylov State scientific center.* Special Issue 2 [in Russian].
14. Droubi, Mohamad & Faisal, Nadimul & Orr, Fraser & Steel, John & El-Shaib, Mohamed (2017) Acoustic emission method for defect detection and identification in carbon steel welded joints. *J. of Constructional Steel Research*, **134**. 10.1016/j.jcsr.2017.03.012.
15. Aboali, Abdalla et al. (2014) Screening for welding defects using acoustic emission technique. *Advanced Materials Research*, **1025–1026**, Trans. Tech. Publ., Ltd., Sept. 2014, 7–12. Crossref. doi:10.4028/www.scientific.net/amr.1025-1026.7.
16. Savchenko, S.V., Timchik, G.S. (2017) Method of control of welded joints on ballistic steels using acoustic emission. *Visnyk NTU KhPI.* Series: Mechanical-technological systems and complexes, Vol. 20 [in Ukrainian].
17. Skalsky, V.R. (2003) Evaluation of accumulation of bulk damage in solid, based on acoustic emission signals. *Tekh. Diagnost. i Nerazrush. Kontrol*, **4**, 29–36 [in Ukrainian].


Received 22.03.2021